

Short Communication

## The Extraction of a Natural Dye Berberine and Evaluation of its Corrosion Inhibition properties for P110SS Steel

Li Na<sup>1,\*</sup>, Guo Hui<sup>1</sup>, Zhao Peng<sup>1</sup>, Zhang Xin<sup>1</sup>, Zhang Lihua<sup>1</sup>, Ambrish Singh<sup>2</sup>

<sup>1</sup> Shaanxi University of Chinese Medicine, the new district of Xian-Xianyang, Shaanxi, 712046, P.R.China.

<sup>2</sup> School of Materials Science and Engineering, Southwest Petroleum University, 8 Xindu district-610500, Chengdu city, Sichuan province, P. R.China.

\*E-mail: [linashaanxi@126.com](mailto:linashaanxi@126.com)

Received: 8 October 2018 / Accepted: 21 November 2018 / Published: 5 January 2019

---

Root extract of *Coptis chinensis* was used to extract berberine a cationic dye to investigate the corrosion inhibition tendency towards P110SS steel in 3.5% NaCl solution containing carbon dioxide. The investigation included electrochemical studies and surface studies. Electrochemical impedance spectroscopy and potentiodynamic polarization methods were used to detect the electrochemical changes at the surface. The surface was explored through scanning electron microscope (SEM), UV-visible, and contact angle methods. The diameter of the Nyquist plots increased with higher concentration of the inhibitor suggesting better inhibition efficiency. The changes in the anodic and cathodic curves suggested both the mechanism were equally modified and therefore the inhibitor was categorized in the mixed type. The SEM images showed the smooth surface of the metal with inhibitor indicating the effective action of the inhibitor on the surface. The UV-visible and contact angle methods also vindicated the effective action of the inhibitor for corrosion of P110SS steel in the aggressive solution. Out of the several isotherms tested for adsorption, Langmuir was found to be the best fit.

---

**Keywords:** Berberine, SEM, UV-Visible, Inhibitor, Corrosion, EIS

### 1. INTRODUCTION

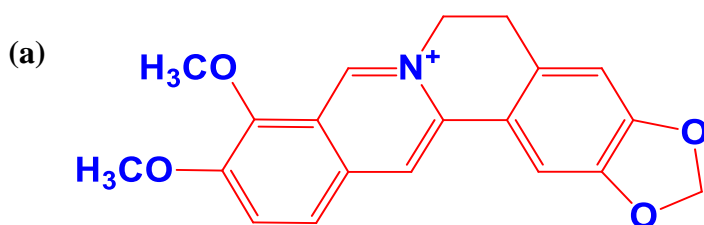
P110SS steel is commonly used in construction industries, oil-gas oil wells, petroleum industries and refineries. P110SS are known for their corrosion resistant properties in the aggressive environment where hydrogen sulphide (H<sub>2</sub>S) is present in abundance. This makes P110SS steel of utmost importance for the tubing and casing steel in reservoir of oil wells where H<sub>2</sub>S is present. Due to its excellent corrosion resistant properties it is also used in construction industries, but it is susceptible to corrosion due to carbon dioxide and marine environment. P110SS finds its place in oil well borings, casing steel

surrounded by concrete material, and in building docks near sea-shore. Even though P110SS steel is useful in sour environment (presence of H<sub>2</sub>S), its corrosion resistant properties are less explored for sweet environment (CO<sub>2</sub>). 3.5% NaCl containing carbon dioxide is an aggressive solution that can cause severe uniform as well as localized corrosion to steels [1, 2].

Deterioration of metals is an environmental process involving electrochemical reactions in presence of water and oxygen. There are many available methods to mitigate corrosion of metals from corrosive environment. Addition of compounds to the reacting environment that can reduce the rate of corrosion is known as inhibition method and the compounds are called inhibitors or mitigators. There are several kinds of inhibitors available. The strict regulations of toxicity control do not allow the use of synthetic/organic inhibitors in large amounts [3]. So, the development of inhibitors based on green principles is always in demand. These are widely used in industries as they are cheap and easy to apply. The inhibitors usually adsorb on the metal surface forming a protective film that prevents the corrosive media to interact with the metal surface. The inhibitor molecules are rich in atoms and functional groups that can form complex and bonds with the vacant orbital of the metals. The intact film of inhibitor on the surface can keep the metal safe for a long period of time till the film is washed away or a crack/scratch appears on the surface [4-8].

The roots of *Coptis chinensis* find an important place in the traditional medicine of China. These roots are very rich in isoquinoline alkaloids berberine, palmatine, hydrastinine and coptisine [9]. Chemical composition of *Coptis chinensis* shows Berberine (5,6-dihydro-9,10-dimethoxybenzo[g]-1,3-benzodioxolo[5,6-a]quinolizinium) as its major constituent which is a strong cationic compound known for its good coloring quality as shown in Figure 1. Due to its coloring quality it is often used as dyes in wools, and cloths. Berberine being a cationic dye extracted from plants is the only one containing isoquinoline alkaloids [10]. The gas chromatography (GC) and infra-red (IR) spectra as shown in Figure 1b and 1c also suggested the presence of pure berberine compound after extraction.

The aim of the present work was to elucidate the inhibition effect of berberine on corrosion of P110SS steel in sweet corrosive media. The investigation was performed using several electrochemical and surface studies.



**Chemical Formula: C<sub>20</sub>H<sub>18</sub>NO<sub>4</sub><sup>+</sup>**

**Molecular Weight: 336.36**

(b)

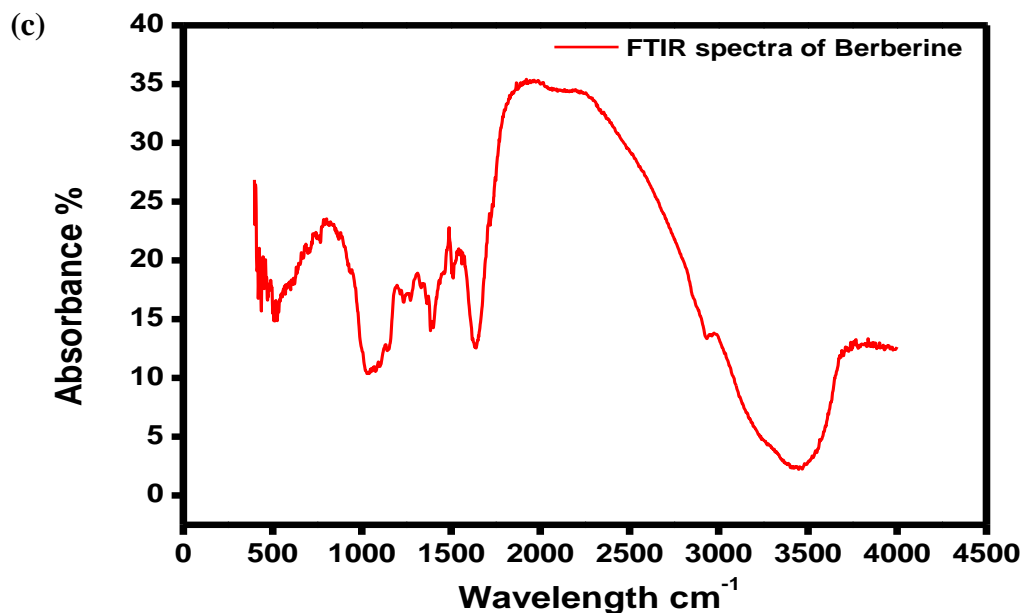
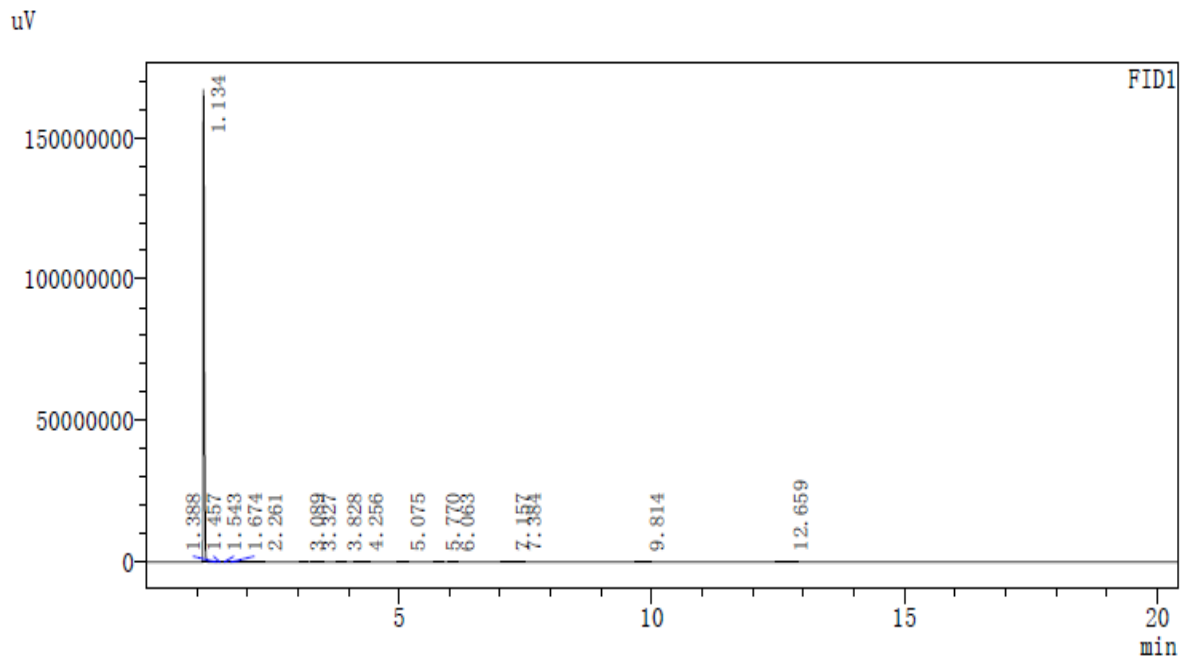


**Figure 1.** (a) Berberine- IUPAC name (5,6-dihydro-9,10-dimethoxybenzo[g]-1,3-benzodioxolo[5,6-a]quinolizinium), (b) GC image of the berberine extract and (c) IR spectra of berberine.

## 2. EXPERIMENTAL

### 2.1. Preparation of Inhibitor

The *Coptis chinensis* roots were purchased from the traditional medicine shop and were completely dried for 7 days. The dried roots were grounded to fine power using a grinder. 50 grams of

powder was dissolved in ethanol to extract Berberine from the roots. The mixture was refluxed and a yellow colored dye was obtained after 5 hours. The dye was then dried using rotary vacuum evaporator. The dye was then refluxed with 3.5% NaCl solution to prepare the solutions which were used for further corrosion studies [11].

## 2.2. Materials and Solutions

All the tests were done using P110SS steel samples which were abraded following the ASTM A262 standard with silicon carbide paper of different grain size [12]. Carbon dioxide was saturated in the 3.5% NaCl solution at a pressure of 5 MPa for 30 minutes and was thoroughly covered with epoxy resin to avoid leakage. The samples were washed repeatedly with water and alcohol to remove any kind of contamination and then dried at room temperature. The specimens were covered with epoxy resin and a 1cm<sup>2</sup> area was used for the electrochemical studies. The corrosive solution of 3.5% NaCl was prepared by using standard sodium chloride diluted with pure refined water [13].

## 2.3. Electrochemical measurements

All the electrochemical experiments were conducted using Autolab workstation. The working electrode, reference electrode, and auxiliary electrode were assembled together in a cell to carry out the reactions at room temperature. The results obtained through experiments were analyzed using FRC software [14]. Before the start of each test an immersion time of 30 minutes was allowed in order to achieve a stable corrosion potential. Impedance experiments were performed in a frequency range from 100 kHz to 0.00001 kHz through amplitude of 10 mV [15]. Usually small amplitude (~10 mV) overlaid on the dc potential can be completely portrayed by the impedance that provides the linear function of the applied perturbation [16].

Potentiodynamic polarization curves were conducted at a scan rate of 1 mV s<sup>-1</sup> and by varying the potential from -300 to +300 mV. The anodic and cathodic plots of the polarization curves were examined to get different parameters. The efficiency of corrosion inhibition was calculated using the following relation [17].

$$\eta\% = \frac{I_{\text{corr}}^{\text{B}} - I_{\text{corr}}^{\text{I}}}{I_{\text{corr}}^{\text{B}}} \times 100 \quad (1)$$

where,  $I_{\text{corr}}^{\text{B}}$  and  $I_{\text{corr}}^{\text{I}}$  are the corrosion current density in lack and in presence of inhibitor. The efficiency of inhibitor as inhibitor was calculated using the charge transfer resistance values as under:

$$\eta\% = \frac{R_{\text{ct}}^{\text{I}} - R_{\text{ct}}^{\text{B}}}{R_{\text{ct}}^{\text{I}}} \times 100 \quad (2)$$

where,  $R_{\text{ct}}^{\text{I}}$  and  $R_{\text{ct}}^{\text{B}}$  are the charge transfer resistance in presence and in absence of inhibitor, respectively [18].

## 2.4. Surface Morphological Studies

### 2.4.1. Contact Angle

To test the hydrophilic and hydrophobic nature of the metal surface contact angle measurements were done using the sessile drop method. All the tests were performed using DSA100 Kruss instrument and prior to each test the samples were cleaned carefully to avoid contaminations [19]. Surface of the metal samples were exposed to the corrosive solution with and without inhibitors for 12 hours. After 12 hours the samples were washed, cleaned and dried before exposing to the Zeiss instrument for SEM tests [20].

### 2.4.2. Scanning Electron Microscopy (SEM)

The P110SS steel samples after the electrochemical tests were washed with acetone to remove the corrosion products and then dried at room temperature. The steel samples were exposed to Zeiss Tescan instrument to get the high resolution images of the surface [21]. Gold spray was also done to get better conductivity and high quality images as the metal samples were small in size.

### 2.4.3. UV-Visible Spectroscopy

The pre solution of Berberine inhibitor and the washing solution of the steel (after 12 hours exposure to Berberine solution) were exposed to UV-5100 double beam spectrophotometer. The change in the peaks of wavelength for pure solution and washing solution were determined for further discussions [22].

## 3. RESULTS AND DISCUSSION

### 3.1. Electrochemical measurements

#### 3.1.1. Electrochemical Impedance Spectroscopy

Impedance studies were carried out to investigate about the redox reaction taking place at the metal surface. The oxidation of P110SS steel due to presence of the corrosive NaCl solution and evaluation of hydrogen provides the description of the reaction taking place at the electrode due to its electrochemical reaction [23, 24]. The transfer of electrons was controlled kinetically as the obtained semicircles of the Nyquist curves are similar in shape as shown in Figure 2 [25]. The high frequency capacitive loop can be observed from the figure that also corresponds to the circuit used to fit the impedance data. The diameter of the capacitive loop becomes bigger with the addition and increase in Berberine concentration. This could be attributed to the roughness at the surface, random active centers, or adsorption of the diverse Berberine molecules [26]. The presence of two times constant in Figure 2a

led to the use of equivalent circuit consisting two times constant shown in Figure 2b. The circuit gave good results with appropriate fits and simultaneous chi square values.

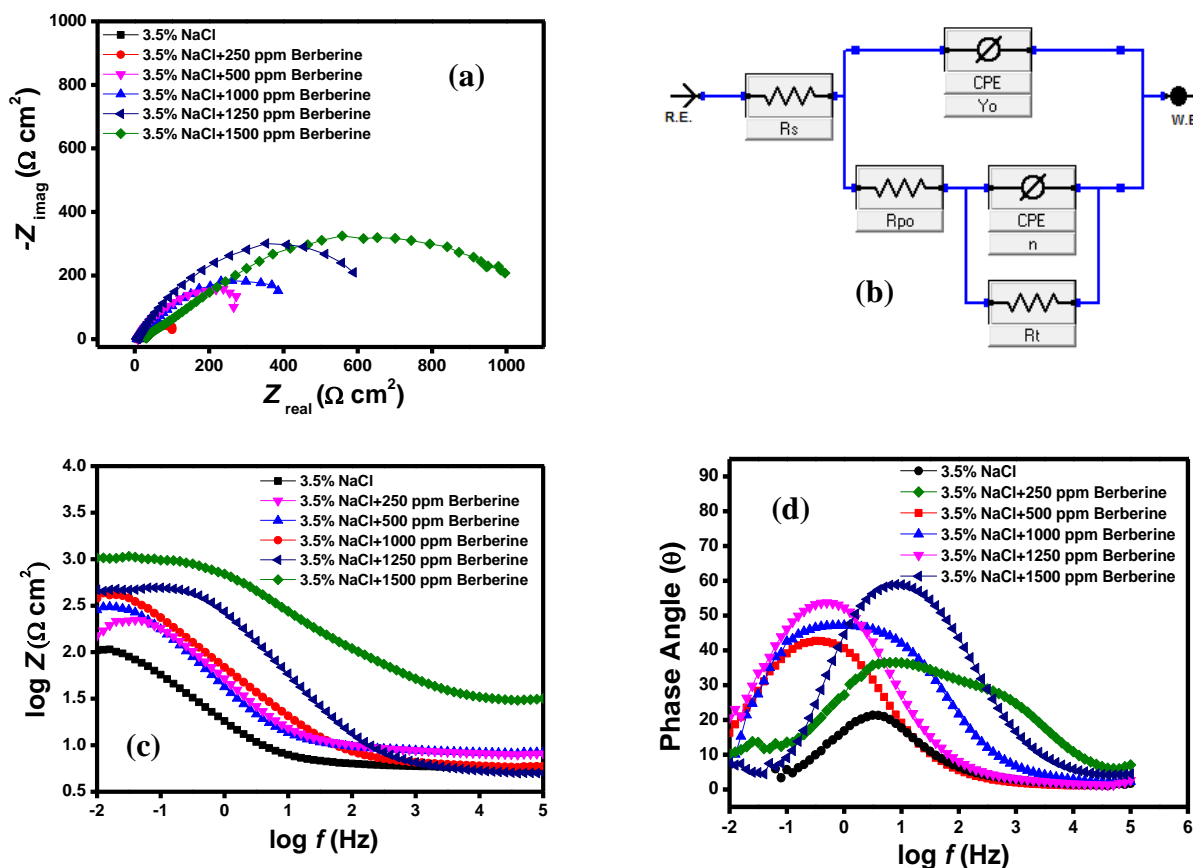


**Figure 2.** (a) Nyquist plots (b) Equivalent circuit used (c) Bode plots and (d) Frequency phase angle plots for P110SS steel in 3.5% NaCl without and with Berberine.

The efficiency of the Berberine for corrosion of P110SS steel was found to increase with increase in the concentration. The increase in charge transfer resistance values as shown in Table 1 is due to the film formed by the Berberine on the surface that increases the resistance to corrosion reaction [27].

**Table 1.** Nyquist data for P110SS steel in 3.5% NaCl for various concentrations of Berberine at 298 K.

Solutions (ppm)	$R_{ct}$ ( $\Omega \text{ cm}^2$ )	$n1$ ( $\Omega^{-1}\text{s}^n/\text{cm}^2$ )	$Y^{\circ 1}$ ( $\Omega^{-1}\text{s}^n/\text{cm}^2$ )	$R_{po}$ ( $\Omega \text{ cm}^2$ )	$n2$ ( $\Omega^{-1}\text{s}^n/\text{cm}^2$ )	$Y^{\circ 2}$ ( $\Omega^{-1}\text{s}^n/\text{cm}^2$ )	$\eta$ %	Surf. coverage $\theta$
3.5% NaCl	20	0.79	0.24	3.1	0.47	0.25	-	-
250 ppm	109	0.82	0.23	3.4	0.56	0.53	81	0.81
500 ppm	261	0.88	0.42	5.6	0.62	0.62	92	0.92
1000 ppm	405	0.89	0.37	6.2	0.78	0.65	95	0.95
1250 ppm	598	0.91	0.32	6.4	0.82	0.71	97	0.97
1500 ppm	994	0.94	0.27	6.7	0.88	0.73	98	0.98

**Table 2.** The slopes of the Bode impedance magnitude plots at intermediate frequencies ( $S$ ) and the maximum phase angles ( $\alpha$ ) for P110SS steel in 3.5% NaCl solution saturated with CO<sub>2</sub> in absence and presence of Berberine.

C (ppm)	-S	$\alpha^\circ$
3.5% NaCl	0.462	19.4
250 ppm	0.579	41.2
500 ppm	0.677	48.5
1000 ppm	0.718	53.6
1250 ppm	0.745	56.7
1500 ppm	0.813	59.8

### 3.1.2. Potentiodynamic polarization measurements

The potentiodynamic polarization curves of the P110SS steel in corrosive media with and without inhibitor are shown in Figure 5. The shift in both anodic and cathodic regions suggested that the corrosion reaction was directed by the transfer of electrons at the electrode surface. Table 1 shows the corrosion potential ( $E_{\text{corr}}$ ), corrosion current density ( $I_{\text{corr}}$ ), and anodic ( $\beta_a$ ) and cathodic ( $\beta_c$ ) slopes evaluated after the polarization tests [28].

The corrosion current density values in Table 3 indicated that the addition of inhibitor to the corrosive system decreases the rate of corrosion. This can be attributed to the complex formed between the inhibitor and the metal that blocks the corrosive media to interact with the electrode surface [29]. The polarization curves for P110SS steel with and without inhibitor are given in Figure 3.

**Table 3.** Tafel polarization data for P110SS steel in 3.5% NaCl for various concentrations of Berberine at 298 K.

Inhibitor	Conc.(ppm)	Tafel data					
		$E_{\text{corr}}$	$I_{\text{corr}}$	$b_a$	$b_c$	$\eta$	$\theta$
		(V vs. SCE)	( $\mu\text{A cm}^{-2}$ )	( $\text{mV d}^{-1}$ )	( $\text{mV d}^{-1}$ )	(%)	
3.5% NaCl	-	-0.690	65	129	92	-	-
Berberine	250 ppm	-0.738	16	96	88	75	0.75
	500 ppm	-0.715	7	57	62	89	0.89

1000 ppm	-0.745	4	73	74	95	0.95
1250 ppm	-0.766	3	63	59	95	0.95
1500 ppm	-0.757	2	68	62	97	0.97

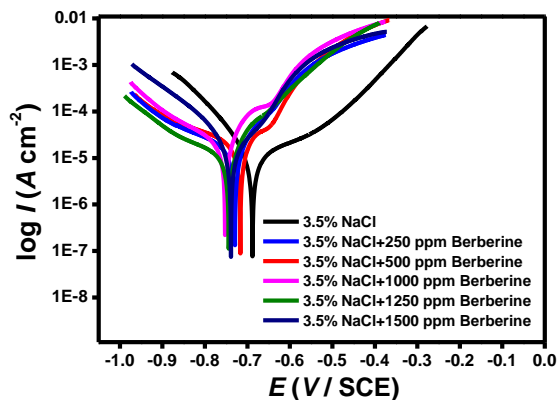


Figure 2. Tafel plots for P110SS steel in 3.5% NaCl in absence and presence of Berberine.

### 3.2. Adsorption isotherm

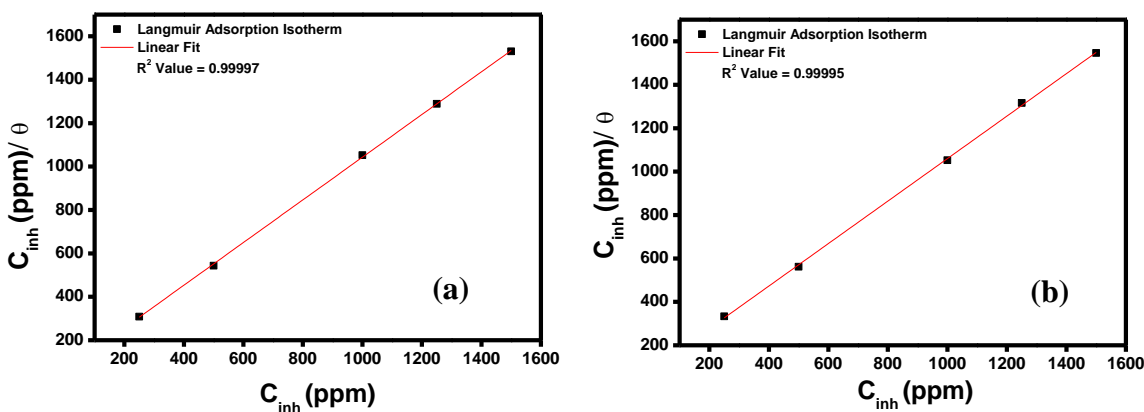


Figure 3. Langmuir isotherms for adsorption of Berberine on P110SS steel surface in 3.5% NaCl (a) Electrochemical impedance spectroscopy (b) Tafel polarization.

The inhibitor molecules tend to adsorb on the metal surface through different mechanisms. A substitutional adsorption reaction between the inhibitor molecules and the water molecules on the surface of metal ( $H_2O_{(ads)}$ ) can be represented as [30].



where,  $x$  is the ratio of size of water molecules that tend to replace the inhibitor molecules on the metal surface [31]. The interaction of inhibitor molecules on the metal surface through adsorption can be studied through several isotherms. Since, the adsorption of inhibitor is a single layer adsorption so the isotherms representing single layer adsorption such as Langmuir, Temkin, and Frenlich were

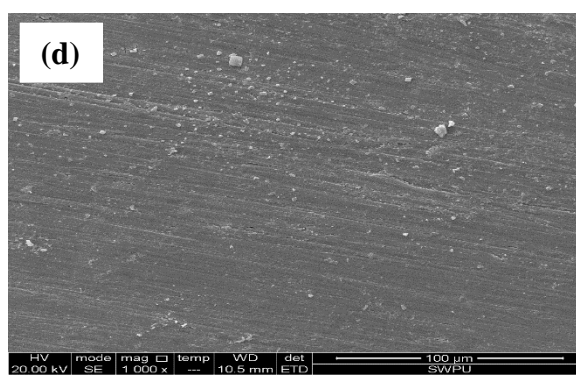
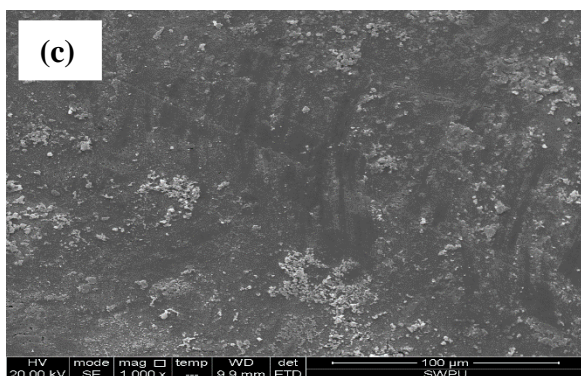
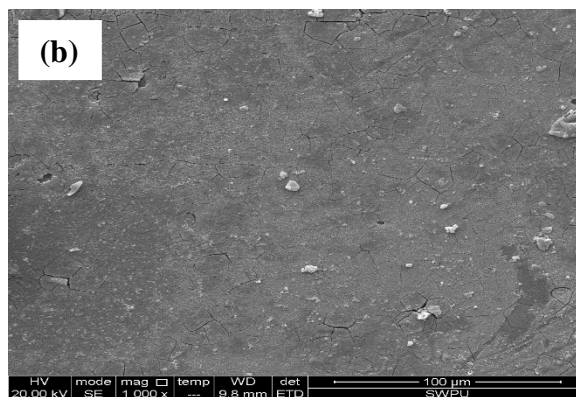
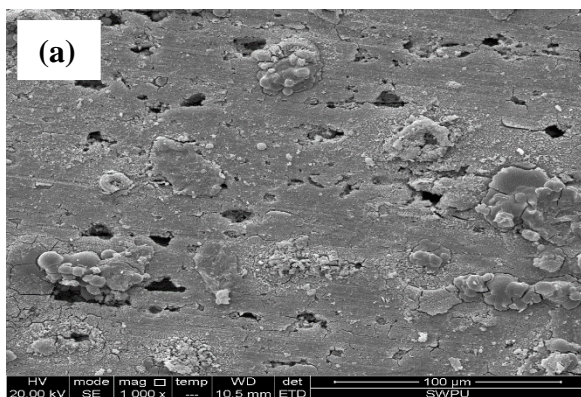
used to study the nature of adsorption. Out of these, Langmuir isotherm provided the best fit results for the adsorption of inhibitor on the metal surface. The linear regression coefficient values ( $R^2$ ) extracted from linear fit result from Langmuir isotherm was in the range of 0.99997 for EIS and 0.99995 for Tafel (Figure 3a, 3b). The relation used to establish Langmuir isotherm is given by the following equation [32].

$$\theta = \frac{bC_{inh}}{1 + bC_{inh}} \quad \text{(Langmuir Isotherm) (4)}$$

### 3.3. Surface Analyses

#### 3.3.1. Scanning Electron Microscopy (SEM)

The P110SS steel samples used in electrochemical experiments were washed with sodium bicarbonate solution followed by acetone to remove the contaminants and the corrosion products. The samples were then dried at room temperature and kept in desiccator [33]. The samples were then taken to the Zeiss Tescan instrument to conduct the tests of the surface to get high resolution micrographs through SEM. The samples were also sprayed with gold for better conductivity of the surface and to get high quality figures. Figure 4a shows the surface of the metal sample that is very corroded and rough in absence of the inhibitor. While in the presence of Berberine the surface of P110SS steel is quite smooth and uniform as shown in Figure 4b, 4c, 4d, 4e and Figure 4f. So, the surface of P110SS steel was less corroded in presence of inhibitor and rough in its absence [34].



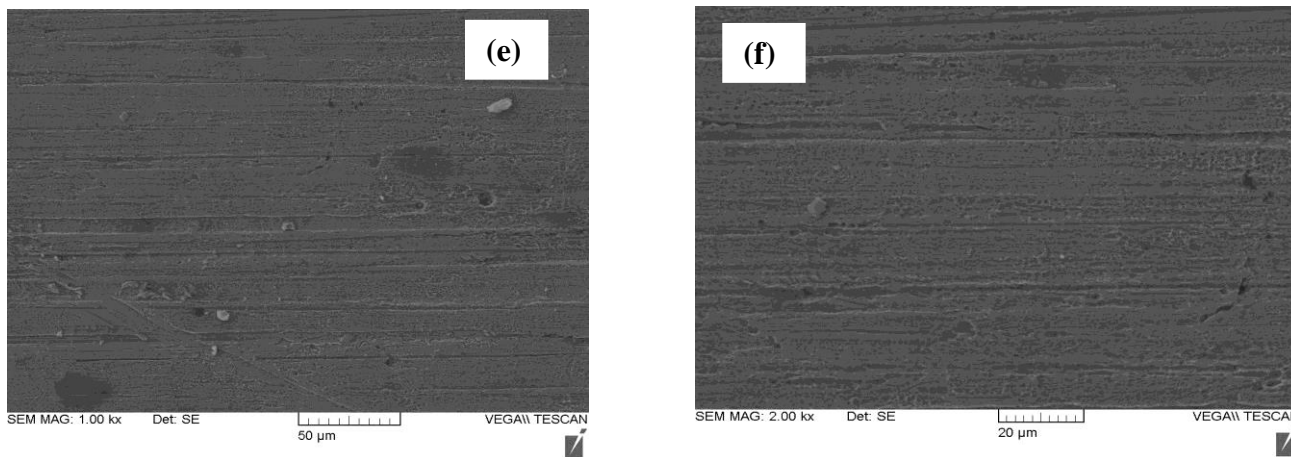


**Figure 4.** SEM images for (a) 3.5% NaCl solution (b) 250 ppm berberine (c) 500 ppm Berberine (d) 1000 ppm Berberine (e) 1250 ppm Berberine and (f) 1500 ppm Berberine.

### 3.3.2. UV-Visible Spectroscopy

The formation of a metal inhibitor complex can be detected by UV-visible spectroscopy. The metal sample was immersed in the pure Berberine solution for 12 hours and then the surface of metal was washed using distilled water. The wavelength of pure solution and the solution obtained after washing the metal surface (washing solution) were recorded. Figure 5 shows the spectrum obtained for both the pure solution and washing solution. The spectrum shows the same shape with variable absorbance indicating the absorbance of pure solution on the metal surface. These changes may arise due to  $\pi$ - $\pi^*$  and n-  $\pi^*$  transitions with a considerable charge transfer character [35].

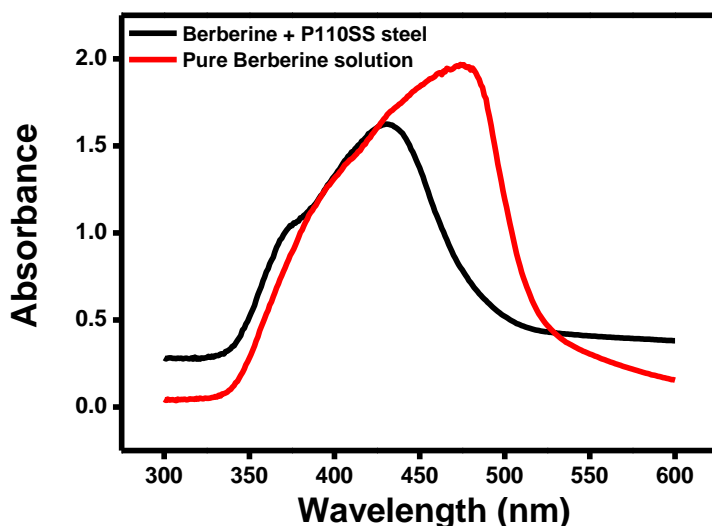


**Figure 5.** UV-Visible spectroscopy of Berberine before and after 12 hours immersion of P110SS steel.

### 3.3.3. Contact Angle

The metal surface can behave as hydrophilic or hydrophobic depending on roughness, presence of corrosion products, and due to films or coatings. The hydrophilic or water loving behavior is usually seen in absence of films when the surface is rough which allows the water to be in direct contact with the surface creating a low contact angle. Whereas, when the surface is smooth or there is a film or coating present then the contact angle tends to be high due to the hydrophobic or water-repelling nature of the metal surface. A baseline was established before the start of each test and the samples were washed repeatedly to avoid contaminations [36]. The aggressive solution was dropped on the surface using sessile method. The metal surface was hydrophilic with contact angle around  $15^\circ$  and became hydrophobic in presence of Berberine film with contact angle of  $68^\circ$ ,  $109^\circ$ ,  $124^\circ$ ,  $128.7^\circ$ , and  $133.4^\circ$ .

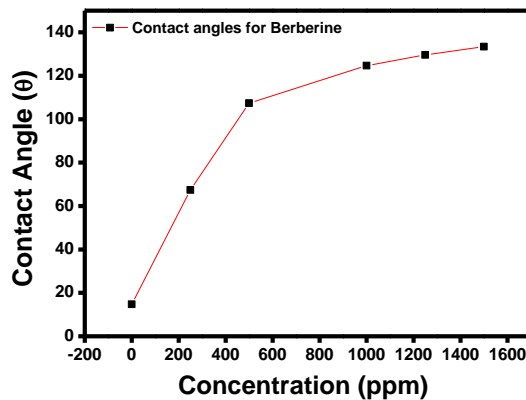


**Figure 5.** Contact angle analysis of Berberine at different concentrations.

## 5. CONCLUSIONS

- The present study showed the protective action of Berberine on P110SS steel surface in 3.5% NaCl solution through electrochemical and surface studies.
- The impedance studies revealed that the charge transfer resistance was found to increase along with the diameter of Nyquist plots with increase in the inhibitor concentration.
- The polarization techniques showed the decrease in corrosion current density values with increase in Berberine concentration leading to better corrosion efficiency. The anodic and cathodic shift in the corrosion potential showed that the inhibitor belong to the mixed category.
- SEM images with smooth surface confirmed the inhibition action of the Berberine on the P110SS steel. Contact angle technique also suggested the insulating action of the Berberine film on the electrode surface.

## ACKNOWLEDGEMENTS

Authors are thankful to the Chinese Medicine and New Drug Research Key Laboratory Project of Shaanxi Province (12JS039, 16JS024) ; The Chinese Medicine Project of Shaanxi Province (ZYMS005). The Shaanxi University of Chinese Medicine Project (14XJZR11)

## References

1. Ambrish Singh, K.R. Ansari, Jiyaul Haque, Parul Dohare, Hassane Lgaz, Rachid Salghi, M.A. Quraishi, *J. Taiwan Inst. Chem. E.*, 82 (2018) 233.
2. A. Singh, K. R. Ansari, X. Xu, Z. Sun, A. Kumar, Y. Lin, *Sci. Report*, 7 (2017) DOI:10.1038/s41598-017-13877-0.
3. G. Gece, *Corros. Sci.*, 53 (2011) 3873.
4. Hong Ju, Yulin Ju, Yan Li, *J. Mater. Sci. Tech.*, 28 (2012) 809.
5. A. Singh, K.R. Ansari, A. Kumar, W. Liu, C. Songsong, Y. Lin, *J. Alloys Comp.*, 712 (2017) 121.
6. Pandian Bothi Raja, Mathur Gopalakrishnan Sethuraman, *Mater. Lett.*, 62 (2008) 113.
7. D. K. Yadav, D. S. Chauhan, I. Ahamad, M. A. Quraishi, *RSC. Adv.*, 3 (2013) 632.
8. A. Singh, E. E. Ebenso, M. A. Quraishi, Y. Lin, *Int. J. Electrochem. Sci.*, 9 (2014) 7495.
9. Hongwei Feng, Ambrish Singh, Yuanpeng Wu, Yuanhua Lin, *New. J. Chem.*, 42 (2018) 11404.
10. Jana Skopalová, JanVacek, Barbora Papoušková, David Jirovský, Vítězslav Maier, Václav Ranc, *Bioelectrochem.*, 87 (2012) 15.
11. A. Singh, Mohd Talha, Xihua Xu, Zhipeng Sun, Yuanhua Lin, *ACS Omega*, 2 (2017) 8177.
12. Songsong Chen, A. Singh, Yuanluqi Wang, Wanying Liu, Kuanhai Deng, Yuanhua Lin, *Int. J. Electrochem. Sci.*, 12 (2017) 782.
13. M. A. Quraishi, A. Singh, V. K. Singh, D. K. Yadav, A. K. Singh, *Mater. Chem. Phys.*, 122 (2010) 114.
14. M. Hazwan Hussin, M. Jain Kassim, N. N. Razali, N. H. Dahon, D. Nasshorudin, *Arab. J. Chem.*, 9 (2016) S616.
15. X. Li, S. Deng, H. Fu, *Corros. Sci.*, 53 (2011) 3241.
16. A. Singh, I. Ahamad, M. A. Quraishi, *Arab. J. Chem.*, 9 (2016) S1584.
17. A. Singh, Y. Lin, W. Liu, D. Kuanhai, J. Pan, B. Huang, C. Ren, D. Zeng, *J. Tai. Inst. Chem. E.*, 45 (2014) 1918.
18. A. Singh, I. Ahamad, V. K. Singh, M. A. Quraishi, *J. Solid State Electrochem.*, 15 (2011) 1087.
19. Hongqiang Wan, Peiyong Han, Shuai Ge, Fancong Li, Simiao Zhang, Huan Li, A. Singh, *Int. J. Electrochem. Sci.*, 13 (2018) 9302.
20. Xihua Xu, A. Singh, Z. Sun, K. R. Ansari, Y. Lin, *R. Soc. Open Sci.*, 4 (2017) 170933.
21. Priyanka Singh, Ambrish Singh, M.A. Quraishi, *J. Taiwan Inst. Chem. E.*, 60 (2016) 588.
22. Zhipeng Sun, Ambrish Singh, Xihua Xu, Songsong Chen, Wanying Liu, Yuanhua Lin, *Res. Chem. Interm.*, 43 (2017) 6719.
23. Chitrasen Gupta, Ishtiaque Ahamad, A. Singh, Xihua Xu, Zhipeng Sun, Yuanhua Lin, *Int. J. Electrochem. Sci.*, 12 (2017) 6379.
24. Ambrish Singh, Y. Lin, W. Liu, S. Yu, J. Pan, C. Ren, D. Kuanhai, *J. Ind. Eng. Chem.*, 20 (2014) 4276.
25. A. Singh, Yuanhua Lin, K. R. Ansari, M. A. Quraishi, E. E. Ebenso, Songsong Chen, W. Liu, *Appl. Surf. Sci.*, 359 (2015) 331.
26. K.R. Ansari, M.A. Quraishi, A. Singh, *Corros. Sci.*, 95 (2015) 62.
27. K.R. Ansari, M.A. Quraishi, A. Singh, *Corros. Sci.*, 79 (2014) 5.
28. Priyanka Singh, Ambrish Singh, M.A. Quraishi, *J. Taiwan Inst. Chem. E.*, 60 (2016) 588.
29. Yan Li, Peng Zhao, Qiang Liang, Baorong Hou, *App. Surf. Sci.*, 252 (2005) 1245.
30. Ambrish Singh, Y. Lin, I. B. Obot, E. E. Ebenso, K. R. Ansari, M. A. Quraishi, *Appl. Surf. Sci.*, 356 (2015) 341.

31. A. Singh, Y. Lin, I. B. Obot. E. E. Ebenso, *J. Mol. Liq.*, 219 (2016) 865.
32. A. Singh, K. R. Ansari, M. A. Quraishi, Hassane Lgaz, Yuanhua Lin, *J. Alloys Comp.*, 762 (2018) 347.
33. A. Singh, Y. Lin, E. E. Ebenso, W. Liu, J. Pan, B. Huang, *J. Ind. Eng. Chem.*, 24 (2015) 219.
34. Yuanhua Lin, Ambrish Singh, E. E. Ebenso, Yuanpeng Wu, Chunyang Zhu, H. Zhu, *J. Tai. Inst. Chem. Eng.*, 46 (2015) 214.
35. K.R. Ansari, M.A. Quraishi, Ambrish Singh, *J. Ind. Eng. Chem.*, 25 (2015) 89.
36. W. Liu, A. Singh, Y. Lin, E. E. Ebenso, G. Tianhan, C. Ren, *Int. J. Electrochem. Sci.*, 9 (2014) 5560.

© 2019 The Authors. Published by ESG ([www.electrochemsci.org](http://www.electrochemsci.org)). This article is an open access article distributed under the terms and conditions of the Creative Commons Attribution license (<http://creativecommons.org/licenses/by/4.0/>).